• Clinical Research •

Functional generalized estimating equation model to detect glaucomatous visual field progression

Sanghun Jeong[1], Hwayeong Kim[2], Sangwoo Moon[3], EunAh Kim[4], Hojin Yang[1], Jiwoong Lee[2,5], Kouros Nouri-Mahdavi[6]

[1]Department of Statistics, Pusan National University, Busan 46241, Republic of Korea
[2]Department of Ophthalmology, Pusan National University College of Medicine, Busan 49241, Republic of Korea
[3]Department of Ophthalmology, Pusan National University Yangsan Hospital, Yangsan 49241, Republic of Korea
[4]Department of Ophthalmology, Samsung Changwon Hospital, Sungkyunkwan University School of Medicine, Changwon 51353, Republic of Korea
[5]Biomedical Research Institute, Pusan National University Hospital, Busan 49241, Republic of Korea
[6]Glaucoma Division, Stein Eye Institute, David Geffen School of Medicine, University of California Los Angeles, Los Angeles, CA 900095, USA
Correspondence to: Hojin Yang. Department of Statistics, Pusan National University, Busan 46241, Republic of Korea. hjyang@pusun.ac.kr; Jiwoong Lee. Department of Ophthalmology, Pusan National University College of Medicine, 179, Gudeok-ro, Seo-gu, Busan 49241, Republic of Korea. glaucoma@pusan.ac.kr
Received: 2025-02-08 Accepted: 2025-05-26

Abstract

● **AIM:** To build a functional generalized estimating equation (GEE) model to detect glaucomatous visual field progression and compare the performance of the proposed method with that of commonly employed algorithms.

● **METHODS:** Totally 716 eyes of 716 patients with primary open angle glaucoma (POAG) with at least 5 reliable 24-2 test results and 2y of follow-up were selected. The functional GEE model was used to detect perimetric progression in the training dataset (501 eyes). In the testing dataset (215 eyes), progression was evaluated the functional GEE model, mean deviation (MD) and visual field index (VFI) rates of change, Advanced Glaucoma Intervention Study (AGIS) and Collaborative Initial Glaucoma Treatment Study (CIGTS) scores, and pointwise linear regression (PLR).

● **RESULTS:** The proposed method showed the highest proportion of eyes detected as progression (54.4%), followed by the VFI rate (34.4%), PLR (23.3%), and MD rate (21.4%). The CIGTS and AGIS scores had a lower proportion of eyes detected as progression (7.9% and 5.1%, respectively). The time to detection of progression was significantly shorter for the proposed method than that of other algorithms (adjusted $P \leq 0.019$). The VFI rate displayed moderate pairwise agreement with the proposed method (k=0.47).

● **CONCLUSION:** The functional GEE model shows the highest proportion of eyes detected as perimetric progression and the shortest time to detect perimetric progression in patients with POAG.

● **KEYWORDS:** functional generalized estimating equation model; primary open angle glaucoma; perimetric progression

DOI:10.18240/ijo.2026.02.12

Citation: Jeong S, Kim H, Moon S, Kim E, Yang H, Lee J, Nouri-Mahdavi K. Functional generalized estimating equation model to detect glaucomatous visual field progression. *Int J Ophthalmol* 2026;19(2):302-311

INTRODUCTION

Glaucoma is a progressive optic neuropathy characterized by glaucomatous optic disc cupping, retinal nerve fiber layer thinning, and visual field loss[1-2]. Standard automated perimetry remains the preferred approach for measuring disease progression in patients with glaucoma[3-5]. Therefore, detecting visual field progression is essential for the timely application of therapeutic intervention to preserve vision in patients with glaucoma[6].

Notably, the observed changes must exceed the expected visual field test-retest variability to detect true perimetric progression[7-8]. Larger intraocular pressure fluctuation, intervening cataract and glaucoma surgery, worse baseline mean deviation (MD), faster visual field decay rate, and higher false positive and false negative rates are associated with increased visual field fluctuation[9].

Numerous approaches have been used to detect visual field progression[10-12]. Event or trend-based methods including glaucoma progression analysis (GPA), rates of MD change,

and rates of visual field index (VFI) change, pointwise linear regression (PLR) analysis, the Advanced Glaucoma Intervention Study (AGIS) score, and Collaborative Initial Glaucoma Treatment Study (CIGTS) score have been suggested to help the clinician to objectively evaluate visual field progression. More recently, deep learning models have been proposed to identify visual field worsening and predict future visual fields[10,13-14]. Yousefi *et al*[15] reported that an automated machine learning system using archetypal analysis identified visual field loss patterns associated with rapid progression in patients with glaucoma. Kim *et al*[16] were able to enhance the detection of visual field progression with a hybrid approach combining archetypal analysis and fuzzy c-means.

Glaucomatous visual field progression is often challenging to detect due to significant test-retest variability and the absence of a universally accepted gold standard for progression assessment. Current methods, such as MD rate and VFI rate, provide global measures of visual field loss but may lack sensitivity to focal defects[17]. Similarly, pointwise regression methods, while capable of detecting localized changes, are prone to false positives due to intrinsic measurement variability[18]. The need for a more reliable approach that integrates spatial and temporal information to enhance sensitivity and specificity remains unmet.

The generalized estimating equation (GEE) model has been applied to estimate diagnostic measures in medical research. Martus *et al*[19] extended the GEE approach to investigate which diagnostic tests should be used as supplementary to each other in eyes with glaucoma. Musch *et al*[20], using a GEE model, found that surgical treatment was more beneficial for patients with advanced visual field loss, while medical treatment was more effective for patients with diabetes. Abe *et al*[21], using a GEE model, found that optical coherence tomography is more effective in detecting glaucoma progression in early stages, while standard automated perimetry is better for advanced stages, with the results influenced by disease severity and number of follow-up visits. Stagg *et al*[22], using a GEE model, found that Black individuals had greater visual field variability than White individuals, delaying glaucoma progression detection.

While previous studies have applied GEE to ophthalmic research, they have primarily utilized scalar covariates, overlooking the spatially correlated structure of visual field data. The proposed functional GEE model extends this approach by incorporating functional covariates, allowing for a more comprehensive assessment of visual field changes over time. This novel methodology enables better differentiation between true disease progression and measurement variability, potentially reducing false-positive rates and improving early detection.

This study aims to develop and validate a functional GEE model for detecting glaucomatous visual field progression. Unlike conventional methods that analyze individual test points or global indices separately, the proposed model accounts for both spatial dependencies and temporal changes in a unified framework. By comparing its performance to widely used progression detection algorithms—including MD rate, VFI rate, PLR, AGIS, and CIGTS score—we evaluate its potential for improving diagnostic accuracy and reducing time to progression detection in clinical practice.

PARTICIPANTS AND METHODS

Ethical Approval This retrospective study was conducted following the principles of the Declaration of Helsinki, and the study protocol was approved by the Institutional Review Board of Pusan National University Hospital (approval number: 2306-033-128). The institutional review board waived the requirement for patient informed consent due to the study's retrospective design.

Study Design and Participants Selection The 6385 visual fields from 716 eyes of 716 patients with primary open angle glaucoma (POAG) who visited glaucoma clinics at Pusan National University Hospital between June 2004 and January 2021 were included in this retrospective, longitudinal, observational study.

The inclusion criteria were age >18y, diagnosis of POAG with five or more visual fields, and a minimum follow-up of 2y. The exclusion criteria included secondary glaucoma including steroid induced glaucoma, pigmentary glaucoma, pseudoexfoliation glaucoma, uveitic glaucoma, neovascular glaucoma, and angle recession glaucoma, uveitis, diabetic retinopathy, age-related macular degeneration, corneal opacity, ocular trauma, and nonglaucomatous optic neuropathies that might affect the visual field. The diagnosis of POAG was based on the following eligibility criteria: 1) presence of glaucomatous optic nerve appearance, corresponding and typical visual field loss; 2) open angles on gonioscopy. Glaucomatous optic neuropathy was defined as having more than a 0.2 cup-to-disc ratio asymmetry between the 2 eyes, neuroretinal rim thinning, notching, or characteristic retinal nerve fiber layer defects indicative of glaucoma. An abnormal visual field was defined as $P<0.05$ for the pattern standard deviation or a glaucoma hemifield test result outside normal limits or a cluster of ≥3 points in the pattern deviation plot in a single hemifield (superior/inferior) with $P<0.05$, one of which must have been $P<0.01$. One eye per individual was randomly selected when both eyes satisfied the inclusion criteria.

The 716 eyes of 716 participants were randomly split into training and test datasets at a ratio of 7:3. There was no patient overlap between the training and test datasets. Totally 501 eyes of 501 patients were included in the method-development

training dataset for the functional GEE model to detect perimetric progression. The 215 eyes of 215 patients were included in the test dataset to evaluate and compare perimetric progression using commonly employed methods.

Baseline Measurements All patients underwent thorough ophthalmologic examination, including best corrected visual acuity, slit-lamp examination, intraocular pressure measurement using Goldmann applanation tonometry, gonioscopy, dilated fundus examination with binocular indirect ophthalmoscopy and slit-lamp biomicroscopy with fundus lens, biometry using the IOL Master (Carl Zeiss Meditec, Dublin, CA, USA), central corneal thickness using ultrasonic pachymetry (Pachmate; DGH Technology, Exton, PA, USA), and keratometry using an auto-kerato-refractometer (ARK-510A; NIDEK, Hiroshi, Japan). Snellen visual acuities were converted to a scale of the logMAR for comparison.

Visual Field Test Automated perimetry was performed using a Humphrey Visual Field Analyzer 750i (Carl Zeiss Meditec Inc.) and a 24-2 or 30-2 Swedish interactive threshold algorithm. Among the 54 test points of the 24-2 test pattern, two physiological scotoma points were excluded, and the remaining 52 test points were used. The 30-2 test pattern was converted into a 24-2 test pattern using the overlapped test points. Reliable visual field tests were defined as a false positive rate <20%, a false negative rate <20%, and fixation loss <33%.

Established Methods for Detecting Visual Field Progression A reference standard for visual field progression was defined as the clinician's assessment of perimetric progression. Three glaucoma specialists (Kim H, Moon S, and Lee J) who were blind to the results of all computational methods clinically assessed each eye. First, pattern deviation (PD) plots were divided into six peripheral (superior and inferior nasal steps and superior and inferior Bjerrum areas) and two paracentral regions[23]. In each peripheral region, a visual field defect is defined as a cluster of at least three adjacent test points corresponding to retinal nerve fiber layer defect with -5 dB or worse for each point. However, a visual field defect is defined as at least two adjacent points with a sum of -15 dB or more for the paracentral region.

Progression was defined in three ways: 1) the presence of a visual field defect in one or more regions in the last visual field, reproduced on a prior visual field but not observed in the baseline visual field; 2) when a visual field defect present in one or more regions on the last two visual fields is worse than that observed in the first two tests (average PD value for all test points in the region worsened by -3 dB or more); or 3) when the average MD values of the final two visual fields was worse by -3 dB or more than the average of the first two visual fields. If the last visual field in the series showed no visual field defects in any regions, the status was defined as no progression. Two glaucoma specialists (Kim H and Moon S) reviewed each visual field series following above mentioned set of criteria. A third glaucoma specialist (Lee J) reviewed all cases of disagreement to reach unanimous decisions.

The AGIS score was calculated for each visual field, as described in the AGIS trial[11]. This score uses the total deviation plot and ranged from 0 to 20, and the scores for each visual field were compared with the baseline scores. An AGIS score increment of at least four points, sustained for three consecutive visual fields, was classified as progression.

The CIGTS score calculation was previously described in the CIGTS trial[11]. This score uses the total deviation probability map and ranged from 0 to 20, and an increment of three or more test points, sustained for three consecutive visual field, was classified as progression.

The MD and VFI slopes were calculated using a simple linear regression of the MD and VFI values for the visual fields. For MD and VFI, visual field progression was defined as a negative slope with a $P<0.05$[11].

For PLR, linear regression was performed for the total deviation values (TDVs) of each of the 52 visual field points. Visual field progression was defined as the presence of any three points with a negative slope ≤-1 dB/year with a $P<0.01$[11].

Statistical Analysis Spatial statistical models mainly focus on random objects measured at grid points (specified by the horizontal and vertical axes). Following Cressie and Wikle[24], spatial data points can be characterized by spatial associations between different locations. Similar to time-series data, spatial data exhibit heteroscedasticity and spatial autocorrelation owing to spatial fluctuations; therefore, the observed data cannot be assumed to be extracted from an independent and homogeneous distribution. Thus, a special approach to analyzing spatial data is required. Let us denote $s_l \in S$ as the grid points associated with the spatial location, where l denotes the l^{th} pixel associated with the location vector S_l and S denotes the entire domain set, that is, $S=\{s_1, s_2, \ldots, s_K\}$. A set of spatial data $\{X^*_{ij}(s_1), X^*_{ij}(s_2), \ldots, X^*_{ij}(s_K)\}$ is observed for the i^{th} subject at the j^{th} visual field examination.

The smoothing process is a statistical method that gives rise to borrowing strength and reinforces the signal by removing noise. This process is used in various fields, including statistical analysis, data analysis, signal processing, image processing, and spatial analysis. We adopted the weighted average method, known as Toba's law, which is widely used in spatial smoothing processes. The primary idea of this smoothing method is to give more weight to observations with a close location and visit time from the given location and visit time, while giving a small weight to observations with a distant location and time within the individual subject. Specifically,

the smoothed observation for the i^{th} subject at the location S_l and time point j is given by

$$X_{ij}(s_l) = \sum_{s_m \in N_{s_l}(h)} \sum_{k \in N_t(\tau)} w^*_{ijkm}(s_l) \cdot X^*_{ik}(s_m)$$

where

$$w^*_{ijkm}(s_l) = \frac{w_{ijkm}(s_l)}{\sum_{s_m \in N_{s_l}(h)} \sum_{k \in N_t(\tau)} w_{ijkm}(s_l)}$$

w_{ijkm} (S_l)=1/2 $N_t(\tau)|(|N_S(h)|$-1) if $k=j$, $m\neq l$, $w_{ijkm}(s_l)$=1/2$|N_t(\tau)|$ if $k\neq j$, $m=l$, $w_{ijkm}(s_l)$=1/2 if $k=j$, $m=l$, and $w_{ijkm}(s_l)$=0 otherwise, for which $N_S(h)$ denotes a set of spatial locations with the spatial lag within some tolerance of h, $N_t(\tau)$ denotes a set of time points with the time lag within some tolerance of τ, and $|N(\cdot)|$ denotes the number of elements in a set $N(\cdot)$. Weights can be set using more flexible kernel functions and various distance metrics; however, we used moving average-type weights in this analysis.

We regarded the smoothed spatial data as functional data and applied a statistical model associated with functional data analysis to the pre-processed data. Functional data refers to data that can be represented as functions over time, space, or other continuous variables. In the functional data analysis, each participant was analyzed as an entire function rather than as an independent value. This allows the examination of characteristics such as patterns in the data, trends, derivatives, and integrals. Liang and Zeger[25] introduced the GEE method to deal with correlated data: the correlation among responses. This has several advantages from a statistical perspective. As mentioned above, the GEE analyzes repeated measurements or clustered data, in which observations are dependent. The GEE is flexible for distributional assumptions and conditions of residuals in that it does not require the assumption of independence and deals with various types of dependent variables (binary, count, and continuous) and the family of generalized linear models. In addition, GEE provides robust standard error estimates. Specifically, the corresponding standard error estimates remain unbiased even if the model is misspecified, that is, the correlation structure is incorrectly specified. Furthermore, the GEE specifies different correlation structures such as independence, exchangeable, and AR (1), making it possible to select the most appropriate correlation structure based on data characteristics. Finally, the estimated regression coefficients in the GEE model can be interpreted similarly to those in the generalized linear models. Therefore, the results are relatively straightforward and easy to understand. For the set of functional data $\{(y_{ij}, X_{ij}(s_1), X_{ij}(s_2),\ldots, X_{ij}(s_K))\}_{i=1,\ldots,n,\ j=1,\ldots,Ti}$, we considered the functional GEE model as follows:

$$g\left(\mathrm{E}(y_{ij})\right) = g(\mu_{ij}) = \beta_0 + \int_S \beta(s)X_{ij}(s)ds,$$

Where $g(\cdot)$ is the link function, β_0 is the intercept, and $\beta(\cdot)$ is a functional coefficient.

Assuming the logit link

$$g(a) = \log\left(\frac{a}{1-a}\right)$$

because of $y_{ij} \in \{0, 1\}$ for all i and j, where the value of zero means nonprogressing and the value of one means progressing, the empirical risk with respect to the negative likelihood function is given by

$$R(\alpha, \beta_0, \beta(\cdot)) = -\frac{1}{n}\sum_{i=1}^{n}\sum_{j=1}^{T_i}\left[y_{ij}\left\{\beta_0 + \int_S \beta(s)X_{ij}(s)ds\right\} - \log\left\{1 + e^{\beta_0 + \int_S \beta(s)X_{ij}(s)ds}\right\}\right].$$

By differentiating the given expression, we obtain the set of GEEs given by

$$\partial_\beta R(\alpha, \beta_0, \beta(\cdot)) = \sum_{i=1}^{n} D_i^T V_i^{-1}(\tilde{y}_i - \tilde{\mu}_i) = 0 \ ,$$

where

$$\mu_{ij} = \Pr(y_{ij} = 1),\ \tilde{y}_i = (y_{i1}, \ldots, y_{iT_i})^T,\ \tilde{\mu}_i = (\mu_{i1}, \ldots, \mu_{iT_i})^T,$$

$$D_i = \mathrm{diag}\left[\mu_{i1}(1-\mu_{i1}), \mu_{i2}(1-\mu_{i2}), \ldots, \mu_{iT_i}(1-\mu_{iT_i})\right]\tilde{X}_i,$$

$$\tilde{X}_i = \{X_{ij}(s_l)\}_{j=1,\ldots,T_i,\ l=1,\ldots,K},\ V_i = B_i^{1/2}R_i(\alpha)B_i^{1/2},$$

$$B_i = \mathrm{diag}\left[\mu_{i1}(1-\mu_{i1}), \mu_{i2}(1-\mu_{i2}), \ldots, \mu_{iT_i}(1-\mu_{iT_i})\right],$$

and $R_i(\alpha)$ is a working correlation matrix with Corr (y_{ij}, $y_{ij'}$)=α if $j\neq j'$ and Corr (y_{ij}, $y_{ij'}$)=1 if $j=j'$.

Therefore, an exchangeable correlation structure was used, because it provides good results under various conditions. We used the TDVs as functional covariates and the number of pixels K was set at K=52. The coefficients and estimated probabilities were calculated by minimizing the empirical risk.

Evaluation Using estimated coefficients, the estimated probability $\hat{\mu}_{ij}$ is given by

$$\hat{\mu}_{ij} = \frac{\exp\left\{\hat{\beta}_0 + \int_S \hat{\beta}(s)X_{ij}(s)ds\right\}}{1 + \exp\left\{\hat{\beta}_0 + \int_S \hat{\beta}(s)X_{ij}(s)ds\right\}}.$$

For each visual field examination of all participants, the optimal cut-off value δ of the estimated probabilities was selected using the receiver operating characteristic (ROC) curve. The optimal cut-off value was selected through Youden's J statistics,

$$\delta = \underset{c}{\mathrm{argmax}}\ J(c) = \underset{c}{\mathrm{argmax}}\ \mathrm{sensitivity}(c) + \mathrm{specificity}(c) - 1,$$

$$\mathrm{sensitivity}(c) = \frac{\sum_{i=1}^{n}\sum_{j=1}^{T_i} I\left(\hat{\mu}_{ij} > c,\ y_{ij} = 1\right)}{\sum_{i=1}^{n}\sum_{j=1}^{T_i} I\left(y_{ij} = 1\right)},$$

$$\mathrm{specificity}(c) = \frac{\sum_{i=1}^{n}\sum_{j=1}^{T_i} I(\hat{\mu}_{ij} < c,\ y_{ij} = 0)}{\sum_{i=1}^{n}\sum_{j=1}^{T_i} I(y_{ij} = 0)}.$$

Table 1 Demographic and ophthalmological characteristics of the entire subjects

Characteristics	Total subjects	Train dataset	Test dataset	*P*
Number of eyes/patients	716/716	501/501	215/215	
Visual field: MD≥-6 dB	441	303	138	0.644[a]
Visual field: -6>MD≥-12 dB	208	150	58	
Visual field: MD<-12 dB	67	48	19	
Age (y)	61.81±14.98	61.63±14.75	62.22±15.53	0.633[b]
Eye, right/left	367/349	254/247	113/102	0.648[a]
Sex, male/female	358/358	260/241	98/117	0.121[a]
Intraocular pressure (mm Hg)	15.91±3.79	15.87±3.66	16.00±4.06	0.668[b]
Axial length (mm)	24.90±1.86	24.97±1.86	24.73±1.85	0.179[b]
Spherical equivalent (diopter)	-2.57±3.56	-2.58±3.45	-2.53±3.82	0.872[b]
Central corneal thickness (μm)	557.73±272.62	553.56±227.93	567.38±355.55	0.551[b]
BCVA (logMAR)	0.11±0.16	0.11±0.17	0.10±0.14	0.803[b]
MD (dB)	-5.60±3.88	-5.67±3.92	-5.46±3.80	0.513[b]
VFI (%)	88.38±11.46	88.30±11.53	88.55±11.30	0.786[b]
PSD (dB)	5.55±3.98	5.55±3.98	5.56±3.99	0.974[b]
Number of visual fields per eye	8.92±3.91	9.05±3.99	8.62±3.74	0.181[b]
Follow-up (y)	5.52±3.16	5.63±3.20	5.24±3.06	0.131[b]

BCVA: Best-corrected visual acuity; logMAR: Logarithm of the minimum angle of resolution; MD: Mean deviation; PSD: Pattern standard deviation; VFI: Visual field index. [a]Chi-squared test; [b]Student *t*-test.

The area under the curve (AUC) was calculated to evaluate the sensitivity and specificity using the optimal cut-off value, δ. Accuracy was also calculated to compare our proposed method with existing methods.

AUC=integral of ROC curve from (0,0) to (1,1)

$$\text{Accuracy} = \frac{TP + TN}{TP + FN + TN + FP},$$

Where *TP* is true positive, *TN* is true negative, *FP* is false positive, and *FN* is false negative.

The proportion of the visual field series identified as progressive was defined as the percentage of progressing eyes determined by each method. Eyes meeting the progression criteria according to a given algorithm at any follow-up visit were defined as progression[26]. There is no gold standard to define visual field progression in patients with glaucoma; therefore, the proportion of series detected as progression is used as a surrogate measure of sensitivity[26].

Time to the first detection of progression was assessed using Kaplan-Meier curves, differences across methods were compared using the log-rank test, and multiple comparisons were adjusted using the Bonferroni test. Furthermore, Cohen's kappa statistic was used to measure a pairwise agreement between the methods[26].

RESULTS

The mean±standard deviation age of the patients at baseline visit, number of visual fields per eye, and follow-up period were 61.81±14.98y, 8.92±3.91 and 5.52±3.16y, respectively (Table 1).

The accuracy (mean±standard deviation) of the functional GEE model in comparison to the clinician's assessment of perimetric progression was 0.750±0.031 [confidence interval (CI)=0.689, 0.811]. However, the accuracy of conventional methods in comparison to the clinician's assessment of perimetric progression were 0.507±0.026 (CI=0.456, 0.559), 0.592±0.027 (CI=0.539, 0.644), 0.527±0.027 (CI=0.474, 0.580), 0.410±0.026 (CI=0.359, 0.462), 0.436±0.028 (CI=0.382, 0.490) for MD, VFI, PLR, AGIS, and CIGTS criteria, respectively (Table 2).

Table 3 shows that the functional GEE model had the highest proportion of eyes detected as progression, followed by the VFI rate, PLR, and MD rate, which had a moderate proportion. However, the CIGTS and AGIS scores had a considerably lower proportion of series detected as progression. The proportion of eyes detected as progression was 54.4%, 34.4%, 23.3%, 21.4%, 7.9%, and 5.1% for the functional GEE model, VFI rate, PLR, MD rate, CIGTS, and AGIS scores, respectively.

Figure 1 showed the cumulative proportion of progressing eyes according to each technique. The time to detect progression was significantly shorter for the functional GEE model compared with that for every other algorithm (adjusted $P \leq 0.019$). However, no other pairwise comparisons were statistically significant. The median (interquartile range) time to detect progression was 905 (479-1435)d, 1500 (919-2018)d, 1542 (965-2019)d, 1617 (1236-2198)d, 1694 (955-2444)d, and 2198 (1351-2468)d for the functional GEE model, VFI rates, MD rates, CIGTS, PLR, and AGIS, respectively.

Table 4 presents the pairwise agreement between the methods. The VFI rate displayed moderate pairwise agreement with the functional GEE model (κ=0.47), while the MD rate and

Table 2 Measures of the accuracy of the different methods

Category (AUC)	Accuracy (mean±SD)	Confidence interval
Functional GEE model (0.803)	0.750±0.031	0.689, 0.811
MD rate	0.507±0.026	0.456, 0.559
VFI rate	0.592±0.027	0.539, 0.644
PLR	0.527±0.027	0.474, 0.580
AGIS	0.410±0.026	0.359, 0.462
CIGTS	0.436±0.028	0.382, 0.490

AGIS: Advanced Glaucoma Intervention Study; AUC: Area under the receiver operating characteristic curve; CIGTS: Collaborative Initial Glaucoma Treatment Study; GEE: Generalized estimating equations; MD: Mean deviation; PLR: Pointwise linear regression; SD: Standard deviation; VFI: Visual field index.

Table 3 Measures of diagnostic properties of the different methods

Status	Functional GEE	MD rate	VFI rate	PLR	AGIS	CIGTS
Progressing	117	46	74	50	11	17
Non-progressing	98	169	141	165	204	198
Detection rate (%)	54.4	21.4	34.4	23.3	5.1	7.9

AGIS: Advanced Glaucoma Intervention Study; CIGTS: Collaborative Initial Glaucoma Treatment Study; GEE: Generalized estimating equations; MD: Mean deviation; PLR: Pointwise linear regression; VFI: Visual field index.

Table 4 Kappa values of the different methods to detect perimetric progression in the test dataset

Items	Functional GEE	MD rate	VFI rate	PLR	AGIS	CIGTS
Reference standard	0.592	0.202	0.424	0.197	0.068	0.106
Functional GEE	NA	0.283	0.47	0.281	0.086	0.117
MD rate	NA	NA	0.55	0.517	0.292	0.3
VFI rate	NA	NA	NA	0.42	0.161	0.18
PLR	NA	NA	NA	NA	0.266	0.306
AGIS	NA	NA	NA	NA	NA	0.543

AGIS: Advanced Glaucoma Intervention Study; CIGTS: Collaborative Initial Glaucoma Treatment Study; GEE: Generalized estimating equations; MD: Mean deviation; PLR: Pointwise linear regression; VFI: Visual field index.

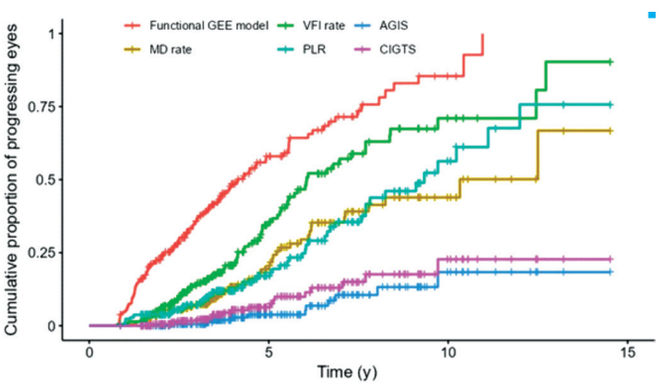

Figure 1 The cumulative proportion of progressing eyes according to each method in the test dataset AGIS: Advanced Glaucoma Intervention Study; CIGTS: Collaborative Initial Glaucoma Treatment Study; GEE: Generalized estimating equations; MD: Mean deviation; PLR: Pointwise linear regression; VFI: Visual field index.

PLR exhibited fair agreement with the functional GEE model (κ=0.283 and κ=0.281, respectively).

Figure 2 showed three representative cases with visual field baseline MD≥-6 dB, in which the functional GEE model detected perimetric progression earlier than other algorithms. In the visual field of November 26, 2019 when the functional GEE model detected perimetric progression, TDV deterioration was apparent in the superior paracentral and nasal step area. These initial changes progressed to obvious superior and inferior visual field defects in the later visual field (Figure 2A). In the visual field of June 30, 2016, when the functional GEE model detected perimetric progression, the deterioration of TDV was apparent in the nasal step area. This initial change became obvious in the later visual field (Figure 2B). In the visual field of September 26, 2017, when the functional GEE model detected perimetric progression, the deterioration of TDV was apparent in the superior paracentral and nasal step area. This initial change became obvious in the later visual field (Figure 2C).

Figure 3 showed three representative cases with visual field baseline MD<-6 dB, in which the functional GEE model detected perimetric progression earlier than other algorithms. In the visual field of October 12, 2018, when the functional GEE model detected perimetric progression, the deterioration of TDV was apparent in the inferior Bjerrum's area. This initial change progressed to an obvious inferior arcuate scotoma in the later visual field (Figure 3A). In the visual field of August 7, 2014, when the functional GEE model detected perimetric

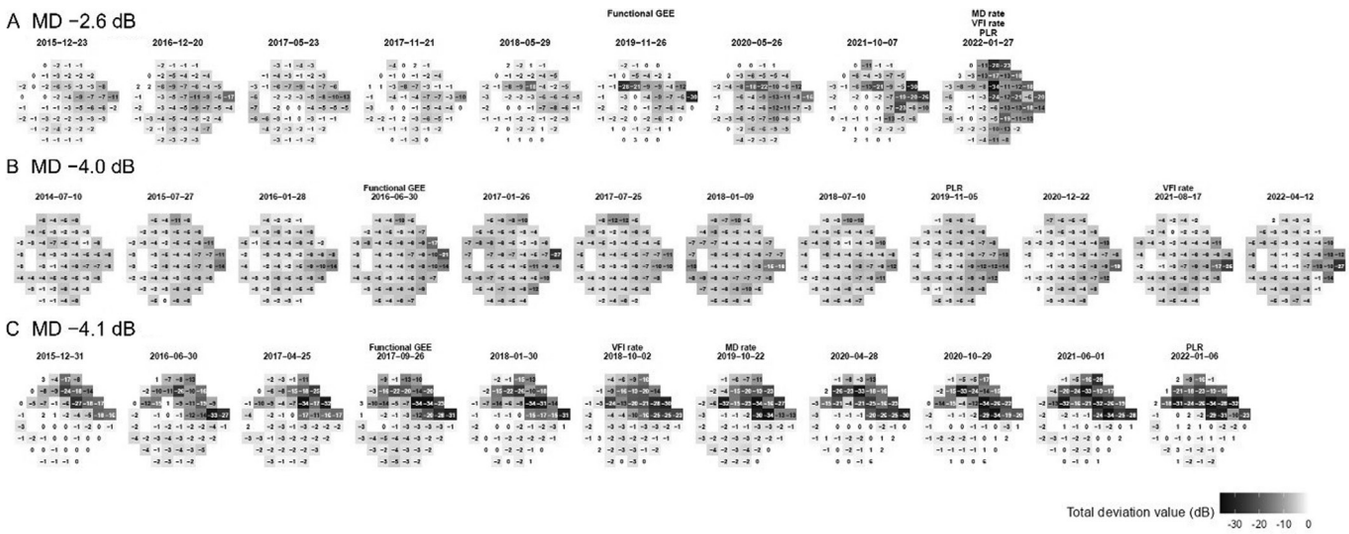

Figure 2 Representative cases with early glaucoma with baseline MD≥-6 dB, in which the functional GEE model detected perimetric progression earlier than other algorithms A: In a 36-year-old female patient, the functional GEE model detected perimetric progression earlier than the MD rate, VFI rate, and PLR analysis; B: In a 22-year-old male patient, the functional GEE model detected perimetric progression earlier than PLR analysis and VFI rate; C: In a 32-year-old female patient, the functional GEE model detected perimetric progression earlier than the VFI rate, MD rate, and PLR analysis. GEE: Generalized estimating equations; MD: Mean deviation; PLR: Pointwise linear regression; VFI: Visual field index.

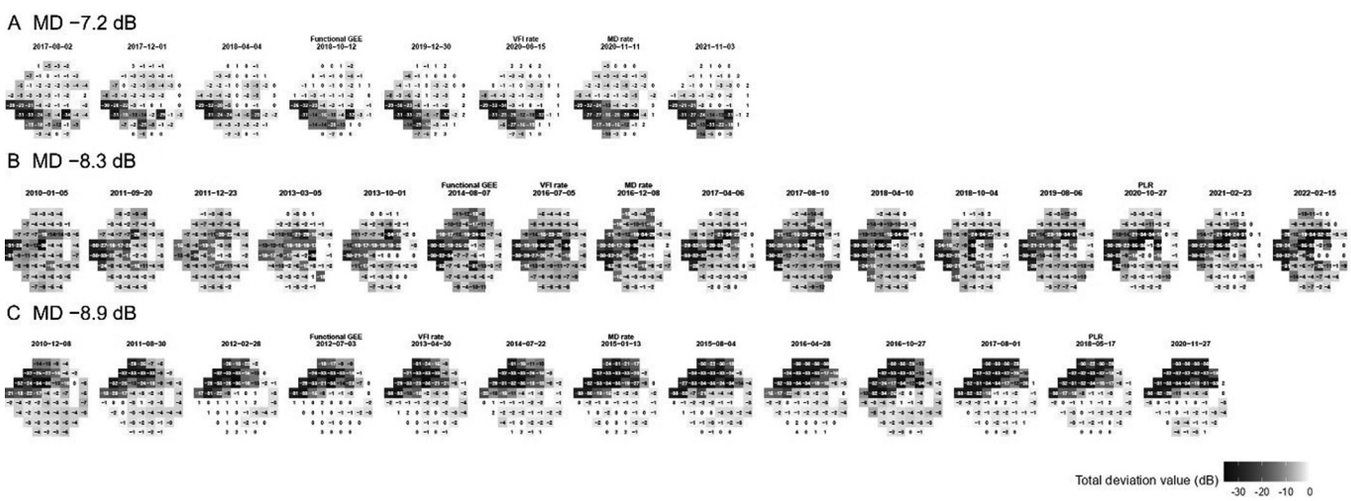

Figure 3 Representative cases with moderate to advanced glaucoma with baseline MD<-6 dB, in which the functional GEE model detected perimetric progression earlier than other algorithms A: In a 49-year-old male patient, the functional GEE model detected perimetric progression earlier than the MD and VFI rate; B: In a 36-year-old female patient, the functional GEE model detected perimetric progression earlier than the VFI rate, MD rate, and PLR analysis; C: In a 33-year-old male patient, the functional GEE model detected perimetric progression earlier than the VFI rate, MD rate, and PLR analysis. GEE: Generalized estimating equations; MD: Mean deviation; PLR: Pointwise linear regression; VFI: Visual field index.

progression, the deterioration of TDV was apparent in the superior and inferior paracentral area. These initial changes progressed to an obvious ring scotoma in the later visual field (Figure 3B). In the visual field of July 3, 2012, when the functional GEE model detected perimetric progression, the deterioration of TDV was apparent in the superior paracentral area. This initial change became an obvious superior altitudinal defect in the later visual field (Figure 3C).

DISCUSSION

We developed a functional GEE model to detect perimetric progression. Compared with existing methods, the functional GEE model had the highest proportion of eyes detected as progression and the earliest detected progression in patients with POAG. The agreement with existing approaches ranged from fair to moderate, except for the AGIS and CIGTS. AGIS and CIGTS had the lowest proportion of eyes detected as progression.

The clinician evaluation graded by a glaucoma specialist based on clearly defined criteria was used as the reference standard to evaluate the accuracy of our functional GEE model[27]. The

accuracy of the functional GEE model (0.750) outperformed that of the MD rate (0.507), VFI rate (0.592), PLR (0.527), CIGTS (0.436), and AGIS (0.410).

Detecting perimetric progression in patients with glaucoma is challenging. Notably, several methods exist for monitoring changes in visual fields; however, no single approach has been universally accepted as the gold standard. Furthermore, using subjective clinician evaluation as a reference standard may underestimate or overestimate the performance of progression detection methods[27]. However, clinician assessment has been widely used as a reference standard to evaluate progression algorithms in previous studies and we used clearly defined criteria for clinician assessment[26-27].

MD and VFI are global indices that summarize mean damage across the entire visual field. However, the MD rate may be insensitive to focal components of visual field deterioration[17]. Furthermore, the VFI provides no spatial information about the visual field and may be insensitive to regional changes or focal components of damage in the same manner[28]. VFI may be less able to detect early glaucomatous change due to the ceiling effect derived from its reliance on pattern deviation probability maps[28]. VFI is heavily weighted towards the central visual field, typically damaged later in the disease, which can also compromise its ability to detect early glaucomatous change[28]. The VFI values become highly variable in serial visual fields of eyes with MDs crossing -20 dB compared with VFIs associated with MDs on either side of -20 dB[29]. In our study, the VFI rate performed better than the MD rate. This may be because VFI is less influenced by cataract and cataract surgery than MD[28]. This finding is consistent with the results of a previous study which reported that the VFI rate performed better than the MD rate in detecting fast-progressors[26].

PLR can effectively detect subtle, localized changes in the visual field that might be missed by global indices such as MD and VFI, making it valuable for identifying focal progression. However, the pointwise sensitivity of visual fields can show considerable variability between tests, leading to a higher false-positive rate of PLR[18]. In the current study, PLR was the slowest to detect progression and performed similarly to the MD rate.

The sensitivity of progression detection of AGIS and CIGTS scores in the current study was lower than that in a previous study[30]. Our study showed that AGIS and CIGTS scores detected the lowest proportion of eyes as progressing disease. Among progressing eyes, 58% and 75% were identified using AGIS and CIGTS criteria, respectively. This could be due to the different follow-up periods in both studies. The mean visual field number for each eye in this study was 8.92 compared with 25 and 22 for the progressing and non-progressing groups, respectively, in the study by Heijl *et al*[30]. AGIS and CIGTS are tailored for more advanced stages of glaucoma; therefore, their scoring systems might not have effectively detected progression in patients with early to moderate glaucoma in our study.

In our cohort of patients, the functional GEE model had the highest proportion of eyes detected as progressing, and it detected progression faster than other methods. The functional GEE model offers several key advantages in detecting visual field progression. 1) Capturing spatial information, which enables us to capture spatial information by reflecting correlation structures in the working correlation matrix. Unlike conventional statistical models that assume independence between observations, GEE accounts for the correlated nature of visual field data by modeling spatial and temporal relationships. This enables the detection of subtle progression patterns that might be missed by global indices such as MD and VFI rates. 2) Interpretability through coefficient estimation: GEE is statistically interpretable because it estimates the coefficients (beta), allowing for the interpretation of the effects of covariates. Therefore, it facilitates clinical decision-making by offering clear insights into the factors influencing progression. 3) Flexibility with link functions: GEE is flexible and can be applied to data from various distributions using different link functions. The flexibility of GEE also allows for the incorporation of different correlation structures, improving model adaptability to various glaucoma severity levels[19,31-33].

Compared to commonly used progression detection methods, the functional GEE model demonstrates superior performance in identifying glaucomatous visual field deterioration. Global indices such as MD and VFI rates lack the ability to capture localized changes, whereas GEE effectively models spatial dependencies to detect focal progression earlier. Similarly, while PLR identifies localized defects, its high false-positive rate can lead to unnecessary clinical interventions; in contrast, GEE improves specificity by incorporating correlation structures across multiple test locations. Furthermore, AGIS and CIGTS scores, although useful for advanced glaucoma, perform poorly in detecting early-stage disease, whereas the proposed model provides a consistent approach across all disease severities. Unlike deep learning-based methods, which require extensive training data and may suffer from interpretability issues, the functional GEE model retains statistical transparency while leveraging functional data analysis to improve detection accuracy.

However, the training process in the GEE requires a sufficiently large sample size, and its computational complexity depends on the sample size, which can lead to prolonged training times, especially in large datasets. Functional GEE is sensitive to the correlation structure selection. The accuracy of the estimates

in the GEE depends on the choice of the working correlation structure[19,31-33].

A previous study revealed a fair-to-moderate level of agreement among methods for detecting visual field progression in patients with glaucoma[26]. The functional GEE model and VFI rate showed moderate agreement, whereas the MD and VFI rates showed the highest agreement. This finding was not unexpected because the two global indices were highly correlated. Therefore, combining multiple methods to detect glaucoma progression can enhance diagnostic accuracy and provide a more comprehensive understanding of disease progression by integrating the strengths of various algorithms and addressing their limitations.

This study has some limitations. The GPA method for progression detection was not included in our study because of the inability to access the data, as GPA is a proprietary software developed by Carl Zeiss Meditec. The reference standard in this study was established based on clinical evaluations of the visual field alone by three glaucoma specialists, without consulting any other clinical data, such as structural optic nerve data. Inspection of serial stereoscopic optic nerve images as a reference standard may improve the performance of our model in progression detection.

In conclusion, the functional GEE approach showed the highest proportion of eyes detected as perimetric progression and the shortest time to detect perimetric progression. Therefore, by identifying patients at a higher risk of glaucoma progression, the proposed functional GEE model may enable clinicians to tailor their treatment plans more effectively and closely monitor changes. This could lead to earlier interventions and potentially better outcomes in preserving vision of patients with glaucoma.

ACKNOWLEDGEMENTS

Authors' Contributions: All authors contributed to the study conception and design. Material preparation, data collection and analysis were performed by Jeong S, Kim H, Moon S, Kim E, Yang H, Lee J. The first draft of the manuscript was written by Jeong S and Lee J and all authors commented on previous versions of the manuscript. All authors read and approved the final manuscript.

Data Availability: The data generated or analyzed during this study are available from the corresponding author upon reasonable request.

Artificial Intelligence Disclosure: We have not used artificial intelligence in the preparation of this manuscript.

Foundations: Supported by the Korea Health Technology R&D Project through the Korea Health Industry Development Institute (KHIDI), funded by the Ministry of Health & Welfare, Republic of Korea (No.HR20C0026); the National Research Foundation of Korea (NRF) (No.RS-2023-00247504); the Patient-Centered Clinical Research Coordinating Center, funded by the Ministry of Health & Welfare, Republic of Korea (No.HC19C0276).

Conflicts of Interest: Jeong S, None; **Kim H,** None; **Moon S,** None; **Kim E,** None; **Yang H,** None; **Lee J,** None; **Nouri-Mahdavi K,** None.

REFERENCES

1 Ju WK, Perkins GA, Kim KY, *et al*. Glaucomatous optic neuropathy: mitochondrial dynamics, dysfunction and protection in retinal ganglion cells. *Prog Retin Eye Res* 2023;95:101136.

2 Schuster AK, Wagner FM, Pfeiffer N, *et al*. Risk factors for open-angle glaucoma and recommendations for glaucoma screening. *Ophthalmologe* 2021;118(Suppl 2):145-152.

3 Chen RI, Gedde SJ. Assessment of visual field progression in glaucoma. *Curr Opin Ophthalmol* 2023;34(2):103-108.

4 Lee GA, Kong GYX, Liu CH. Visual fields in glaucoma: where are we now *Clin Exp Ophthalmol* 2023;51(2):162-169.

5 Susanna FN, Melchior B, Paula JS, *et al*. Variability and power to detect progression of different visual field patterns. *Ophthalmol Glaucoma* 2021;4(6):617-623.

6 Huang J, Galal G, Mukhin V, *et al*. Prediction and detection of glaucomatous visual field progression using deep learning on macular optical coherence tomography. *J Glaucoma* 2024;33(4):246-253.

7 Tan JCK, Agar A, Kalloniatis M, *et al*. Quantification and predictors of visual field variability in healthy, glaucoma suspect, and glaucomatous eyes using SITA-faster. *Ophthalmology* 2024;131(6):658-666.

8 Choi EY, Li D, Fan YY, *et al*. Predicting global test-retest variability of visual fields in glaucoma. *Ophthalmol Glaucoma* 2021;4(4):390-399.

9 Rabiolo A, Morales E, Kim JH, *et al*. Predictors of long-term visual field fluctuation in glaucoma patients. *Ophthalmology* 2020;127(6):739-747.

10 Dixit A, Yohannan J, Boland MV. Assessing glaucoma progression using machine learning trained on longitudinal visual field and clinical data. *Ophthalmology* 2021;128(7):1016-1026.

11 Sabharwal J, Hou KH, Herbert P, *et al*. A deep learning model incorporating spatial and temporal information successfully detects visual field worsening using a consensus based approach. *Sci Rep* 2023;13(1):1041.

12 Marín-Franch I, Artes PH, Turpin A, *et al*. Visual field progression in glaucoma: comparison between PoPLR and ANSWERS. *Transl Vis Sci Technol* 2021;10(14):13.

13 Kim H, Lee J, Moon S, *et al*. Visual field prediction using a deep bidirectional gated recurrent unit network model. *Sci Rep* 2023;13:11154.

14 Lee J, Park K, Kim H, *et al*. Bidirectional gated recurrent unit network model can generate future visual field with variable number of input elements. *PLoS One* 2024;19(8):e0307498.

15 Yousefi S, Pasquale LR, Boland MV, *et al*. Machine-identified patterns of visual field loss and an association with rapid progression in the ocular hypertension treatment study. *Ophthalmology* 2022;129(12):1402-1411.

16 Kim H, Moon S, Lee J, *et al*. Fuzzy clustering of 24-2 visual field patterns can detect glaucoma progression. *PLoS One* 2024;19(9):e0309011.

17 Mahmoudinezhad G, Lin M, Rabiolo A, *et al*. Rate of visual field decay in glaucomatous eyes with acquired pits of the optic nerve. *Br J Ophthalmol* 2021;105(3):381-386.

18 De Moraes CG, Liebmann CA, Susanna R Jr, *et al*. Examination of the performance of different pointwise linear regression progression criteria to detect glaucomatous visual field change. *Clin Exp Ophthalmol* 2012;40(4):e190-e196.

19 Martus P, Stroux A, Jünemann AM, *et al*. GEE approaches to marginal regression models for medical diagnostic tests. *Stat Med* 2004;23(9):1377-1398.

20 Musch DC, Gillespie BW, Lichter PR, *et al*. Visual field progression in the Collaborative Initial Glaucoma Treatment Study the impact of treatment and other baseline factors. *Ophthalmology* 2009;116(2):200-207.

21 Abe RY, Diniz-Filho A, Zangwill LM, *et al*. The relative odds of progressing by structural and functional tests in glaucoma. *Invest Ophthalmol Vis Sci* 2016;57(9):OCT421-OCT428.

22 Stagg B, Mariottoni EB, Berchuck S, *et al*. Longitudinal visual field variability and the ability to detect glaucoma progression in black and white individuals. *Br J Ophthalmol* 2022;106(8):1115-1120.

23 Loomis SJ, Kang JH, Weinreb RN, *et al*. Association of CAV1/CAV2 genomic variants with primary open-angle glaucoma overall and by gender and pattern of visual field loss. *Ophthalmology* 2014;121(2):508-516.

24 Cressie N, Wikle CK. Statistics for spatio-temporal data. *John Wiley & Sons* 2011;P243-P296.

25 Liang KY, Zeger SL. Longitudinal data analysis using generalized linear models. *Biometrika* 1986;73(1):13-22.

26 Rabiolo A, Morales E, Mohamed L, *et al*. Comparison of methods to detect and measure glaucomatous visual field progression. *Transl Vis Sci Technol* 2019;8(5):2.

27 Wang MY, Shen LQ, Pasquale LR, *et al*. An artificial intelligence approach to detect visual field progression in glaucoma based on spatial pattern analysis. *Invest Ophthalmol Vis Sci* 2019;60(1):365-375.

28 Artes PH, O'Leary N, Hutchison DM, *et al*. Properties of the statpac visual field index. *Invest Ophthalmol Vis Sci* 2011;52(7):4030-4038.

29 Lee JM, Cirineo N, Ramanathan M, *et al*. Performance of the visual field index in glaucoma patients with moderately advanced visual field loss. *Am J Ophthalmol* 2014;157(1):39-43.

30 Heijl A, Bengtsson B, Chauhan BC, *et al*. A comparison of visual field progression criteria of 3 major glaucoma trials in early manifest glaucoma trial patients. *Ophthalmology* 2008;115(9):1557-1565.

31 Hanley JA, Negassa A, Edwardes MD, *et al*. Statistical analysis of correlated data using generalized estimating equations: an orientation. *Am J Epidemiol* 2003;157(4):364-375.

32 Paul S, Zhang XM. Small sample GEE estimation of regression parameters for longitudinal data. *Stat Med* 2014;33(22):3869-3881.

33 Twisk JWR. Longitudinal data analysis. a comparison between generalized estimating equations and random coefficient analysis. *Eur J Epidemiol* 2004;19(8):769-776.